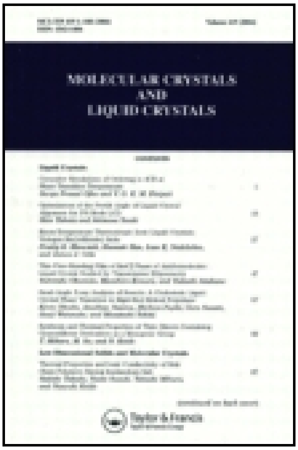

Molecular Crystals and Liquid Crystals Science and Technology. Section A. Molecular Crystals and Liquid Crystals

Publication details, including instructions for authors and subscription information:
http://www.tandfonline.com/loi/gmcl19

Electro-Optical and Dielectric Investigations of Antiferroelectric and Ferrielectric Smectic Phases

G. Heppke [a], D. Lötzsch [a], J. Nolte-Bömelburg [a] & S. Rauch [a]

[a] Iwan-N.-Stranski Institut, Sekr. ER11, Technische Universität Berlin, Straße des 17. Juni 135, 10623, Berlin, Germany

Version of record first published: 04 Oct 2006

Mol. Cryst. Liq. Cryst., Vol. 317, pp. 65–82
Reprints available directly from the publisher
Photocopying permitted by license only

Electro-Optical and Dielectric Investigations of Antiferroelectric and Ferrielectric Smectic Phases*

G. HEPPKE**, D. LÖTZSCH, J. NOLTE-BÖMELBURG and S. RAUCH

Iwan-N.-Stranski Institut, Sekr. ER11, Technische Universität Berlin, Straße des 17. Juni 135, 10623 Berlin, Germany

(Received in final form 28 September 1996)

Dielectric and electro-optical properties of the various antiferroelectric and ferrielectric smectic phases of two compounds of the homologous series MHP*n*CBC ($n=8,9$) have been investigated. MHP9CBC exhibits an unidentified chiral induced SmC subphase (denoted by SmC_X^*) and shows the phase sequence Cr – SmI_A^* – SmC_A^* – SmC_γ^* – SmC_X^* – SmC_X^* – SmA – I. The electro-optical and dielectric properties of the SmC_X^* phase of MHP9CBC differ distinctly from that of the SmC_α^* as well as the SmC_γ^* phase. The electric field – temperature phase diagram was obtained by two methods, measurement of the apparent tilt angle as well as the dielectric loss. The results of both methods are in good agreement. For both compounds a field induced ferrielectric state is observed in a broad temperature range ($\approx$ 10 K) of the SmC_A^*-phase.

Keywords: Antiferroelectric liquid crystals; SmC subphases; electro-optical studies; dielectric properties; antiferroelectricity; ferrielectricity

INTRODUCTION

Soon after the discovery of antiferroelectricity in chiral smectic liquid crystals in 1989 [1] several additional SmC subphases have been found. Besides the alternating tilted SmC_A phase which shows antiferroelectric behaviour (e.g., tristate switching) [2, 3] if composed of chiral molecules, MHPOBC was found to exhibit three tilted smectic phases in a narrow temperature range between SmA and SmC_A^* phase (the SmC_α^* phase [4, 5],

* Presented in part at the 16th Int. Liq. Cryst. Conf., Kent (Ohio), 1996.
**Corresponding author.

the ferrielectric SmC^*_γ phase [4] and the SmC^*_β phase which is probably of identical structure as the SmC* phase [1]).

Since that time a large number of compounds exhibiting the alternating tilted SmC^*_A phase as well as a variety of SmC* subphases with ferrielectric and antiferroelectric properties have been synthesized and their physical properties investigated [6]. For the SmC* phase and the SmC^*_A phase the existing structural models are able to explain the observed characteristic physical behaviour quite well. On the other hand the structures of the different SmC* subphases reported in literature (SmC^*_α, SmC^*_γ, SmC^*_{FI1}, SmC^*_{FI2}, AF*) are not quite clear up to now [5, 6, 7]. Therefore it is of great interest to perform further studies on materials with a broad temperature range of the different ferri- and antiferroelectric phases. Most experimental investigations carried out on these phases are restricted to either electro-optical measurements or dielectric spectroscopy, which makes it difficult to compare the results obtained by the different experimental methods.

In this contribution we report detailed electro-optical and dielectric investigations of two members of a homologous series of antiferroelectric liquid crystals. The homologue MHP8CBC [8] exhibits a direct SmC^*_A to SmC^*_α phase transition (SmI^*_A – SmC^*_A – SmC^*_α – SmA) whereas for compound MHP9CBC two additional SmC subphases (SmC^*_γ and an unidentified phase denoted as SmC^*_x) are observed between the SmC^*_A and the SmC^*_α phase.

Special attention is paid to the electric field dependence of the dielectric spectra and the apparent tilt angle of the chiral induced SmC subphases. The results enable us to construct electric field – temperature phase diagrams for both compounds.

SUBSTANCES UNDER INVESTIGATION

Phase sequences and transition temperatures of MHP*n*CBC ($n = 8, 9$) are given below. Compound MHP8CBC has been described earlier in literature [8]. Its transition temperatures are in good agreement with this reference.

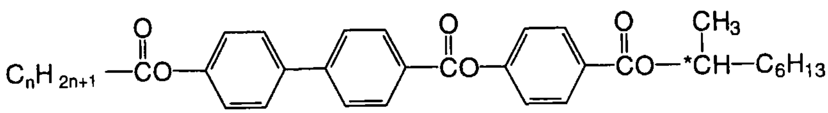

(MHPnCBC)

TABLE I Polymorphism and transition temperatures of MHP*n*CBC (n = 8, 9)

n	Cr	SmI^*_A	SmC^*_A	SmC^*_γ	SmI^*_x	SmC^*_α	SmA	I
8	• 77.9	(• 73)	• 100.5	–	–	• 106.5	• 148.1	•
9	• 57.3	• 68	• 106.8	• 108.5	• 109.3	• 113.5	• 144.6	•

In order to classify the smectic phases of (S)-MHP9CBC we performed miscibility studies with (S)-MHPOBC as reference compound (see Fig. 1). The SmI^*_A, SmC^*_A, SmC^*_γ, SmC^*_α and SmA phases of (S)-MHPOBC are uninterrupted miscible with the respective phases of (S)-MHP9CBC proving the isomorphism of these phases. Only the SmC^*_x phase of (S)-MHP9CBC is not miscible with any of the phases of (S)-MHPOBC.

As can be seen in Figure 2 the SmC^*_x phase is induced by chirality. Similar to the SmC^*_γ and SmC^*_α phases it disappears below an enantiomeric excess of approximately 70%. In order to obtain more information about the SmC^*_x phase we carried out detailed measurements of the apparent tilt angle and the dielectric properties of MHP9CBC in the different SmC subphases.

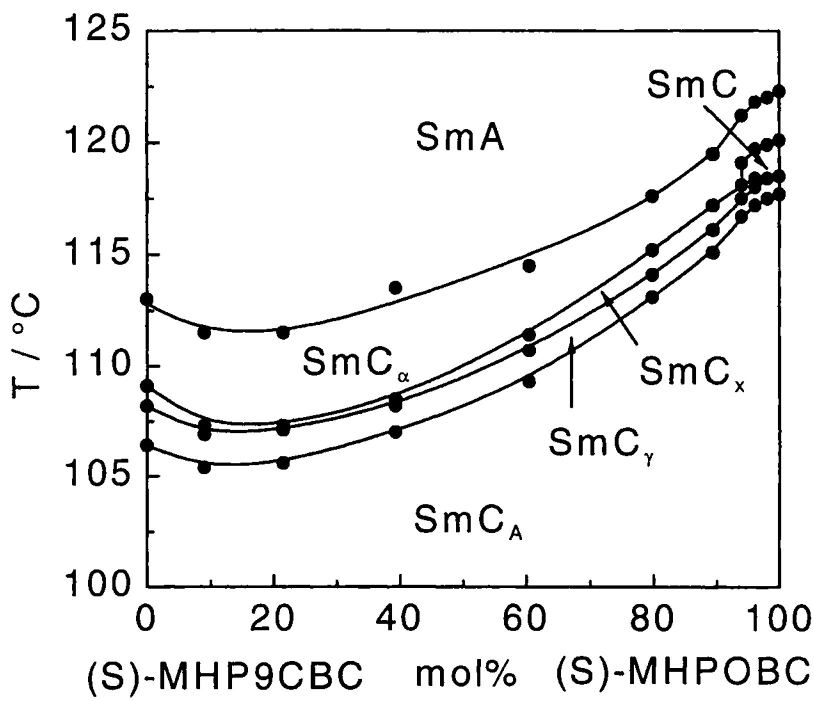

FIGURE 1 Binary phase diagram between (S)-MHP9CBC and (S)-MHPOBC.

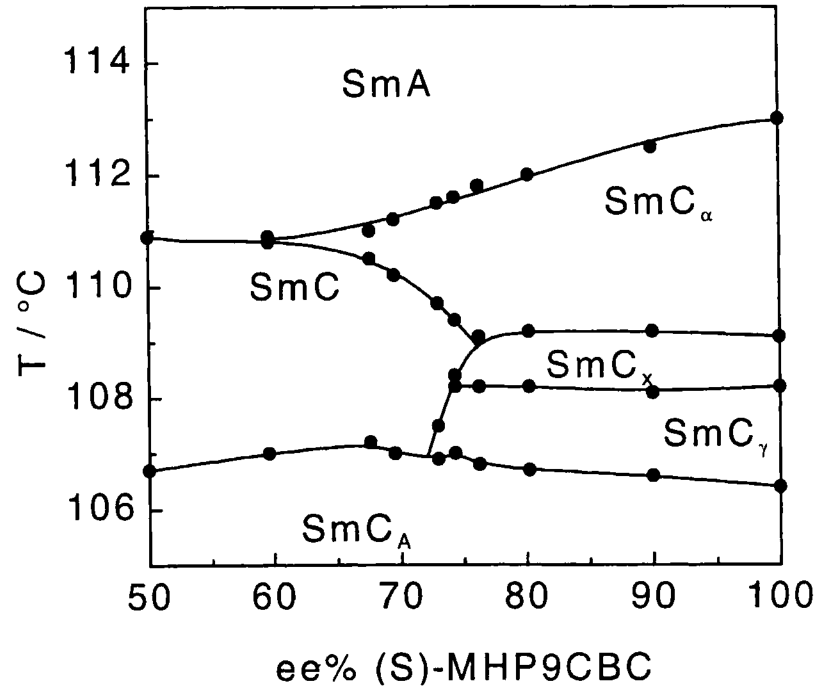

FIGURE 2 Phase transition temperatures of MHP9CBC as a function of enantiomeric excess.

EXPERIMENTAL

For electro-optical and dielectric measurements commercially available (EHC) test cells (ITO, rubbed polyimid) with a cell gap of about 4 μm or 10 μm and an electrode area of 16 mm^2 were used. The exact spacing was determined by measuring the capacitance of the empty cell. After filling homogeneous planar alignment was achieved by slowly cooling from the isotropic phase (cooling rate: 0.1 K/min) under application of a triangular electric field of high field strengths (up to 30 V/μm) and different frequencies (frequency range: 10–100 Hz). Alignment could be further improved by using the same method in the SmC_A^* phase. For temperature control we used a heating stage with an accuracy of 0.1 K. Values of the polarization were obtained by using the Diamant bridge method. For measurements of the apparent tilt angle a DC electric field was applied. The switching angle was then obtained by determining the minimum of the transmitted light (detected by a photomultiplier) when rotating the crossed polarizers. For dielectric spectroscopy a LC meter has been used. The amplitude of the measuring AC field has been 0.5 V_{rms} with an additionally applied DC voltage of 0 up to 40 V.

RESULTS

The apparent tilt as a function of applied electric field is shown on the left hand side of the following figures for the different SmC* subphases of MHP9CBC (SmC^*_α: 110°C, SmC^*_γ: 107.5°C and SmC^*_x: 108.5°C) and MHP8CBC (SmC^*_α: 102°C). Values have been taken for increasing as well as decreasing voltage in order to reveal the hysteresis behaviour of the apparent tilt. On the right hand side the dielectric loss versus applied DC electric field and frequency is depicted for the same temperatures. For clarity of the figures the dielectric spectra are shown only for decreasing voltage.

SmC^*_α Phase

In the SmC^*_α phase of MHP9CBC at 110°C a hysteresis free tristate switching with a well defined threshold field is observable as shown in Figure 3. This switching behaviour is reflected in the dielectric spectrum (Fig. 4) by a discontinuous decrease of the dielectric loss when reaching the threshold voltage. At lower values of the electric field a linear effect with surprisingly high values of Θ/E (of about 2.5 deg $\cdot$ V^{-1} $\cdot$ μm). is observed.

In the SmC^*_α phase of MHP8CBC a similar dependence of the apparent tilt on the applied electric field is observed (Fig. 5). At 102°C a threshold field of about 2.2 V $\cdot$ μm^{-1} and an apparent tilt angle of about 9 deg have been measured. Below the threshold field a value of Θ/E of about 1.6 deg $\cdot$ V^{-1} $\cdot$ μm is found. At the temperature of 102°C there exists a distinct difference in the dielectric behaviour of MHP8CBC (Fig. 6) when compared with the optical tilt. Whereas the apparent tilt shows a dicontinuous decrease of about 6° at the transition from the homogeneously tilted state to the SmC^*_α state in the dielectric spectra a nearly continuous decrease of the dielectric strength with increasing DC electric field is observed (as also reported in literature [7]). The field induced transition ($E \approx 2.2$ V $\cdot$ μm^{-1}) is only indicated by a small rise in the dielectric strength.

Assuming a short pitch helicoidal structure for the SmC^*_α phase there should exist a Goldstone mode (with strong contribution especially in the low temperature region) and a softmode (with strong contribution in the high temperature region) [7]. Both processes contribute to the dielectric strength exhibiting a relaxation process in nearly the same frequency region.

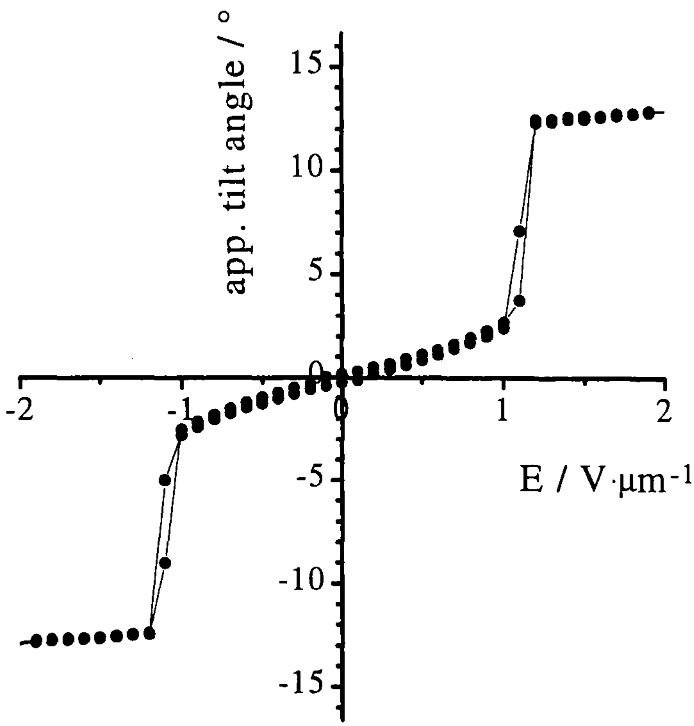

FIGURE 3 Apparent tilt angle of MHP9CBC as a function of electric field in the SmC^*_α (at 110°C).

In the middle of the temperature region of the SmC^*_α phase one can expect to observe a mixture of both processes. Measuring the dependence of dielectric strength on the electric field the soft mode part should be affected only little by the electric field whereas the Goldstone mode part should vanish at a distinct threshold. Depending on temperature and probably also on the phase sequence either a stepwise change in dielectric strength (as can be seen in Fig. 4) or a more or less continuous decrease (Fig. 6) are observable.

SmC^*_γ Phase

Typical ferrielectric properties are observed for the SmC^*_γ phase (Figs. 7 and 8). Helical unwinding takes place at low electric field strength (approximately 1 $V \cdot \mu m^{-1}$) leading to an unwound ferrielectric state with a value of apparent tilt of about one third of the saturated tilt. Unwinding of the helical structure is connected with the disappearance of the ferrielectric

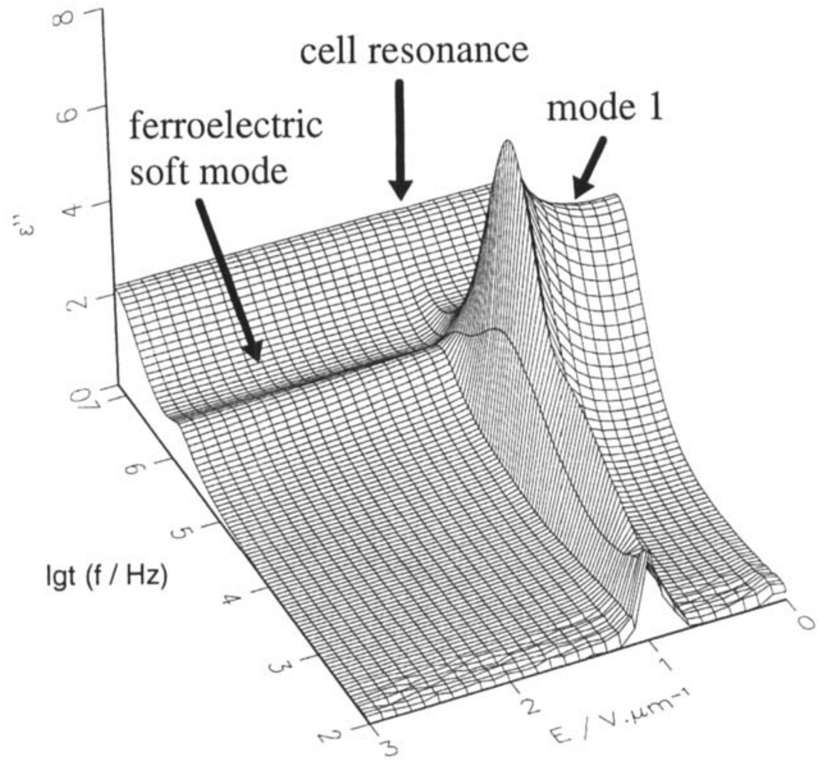

FIGURE 4 Dielectric loss of MHP9CBC versus frequency and electric field strength in the SmC_{α}^{*} phase (at 110°C).

Goldstone mode (high absorption at low frequency) in the dielectric spectra. Only very small relaxation processes which are not visible in Figure 8 are observable in the region of the ferrielectric state. When further increasing the electric DC field a homogeneous tilted SmC state is reached exhibiting a small dielectric absorption process which is due to the ferroelectric soft mode.

SmC_{x}^{*} Phase

Unusual electro-optical and dielectric properties are observed for the SmC_{x}^{*} phase as shown in Figures 9 and 10. Like in the SmC_{γ}^{*} phase there exists a step at low electric field which again is probably due to helical unwinding. However the apparent tilt angle is smaller than 1/3 of the saturated value.

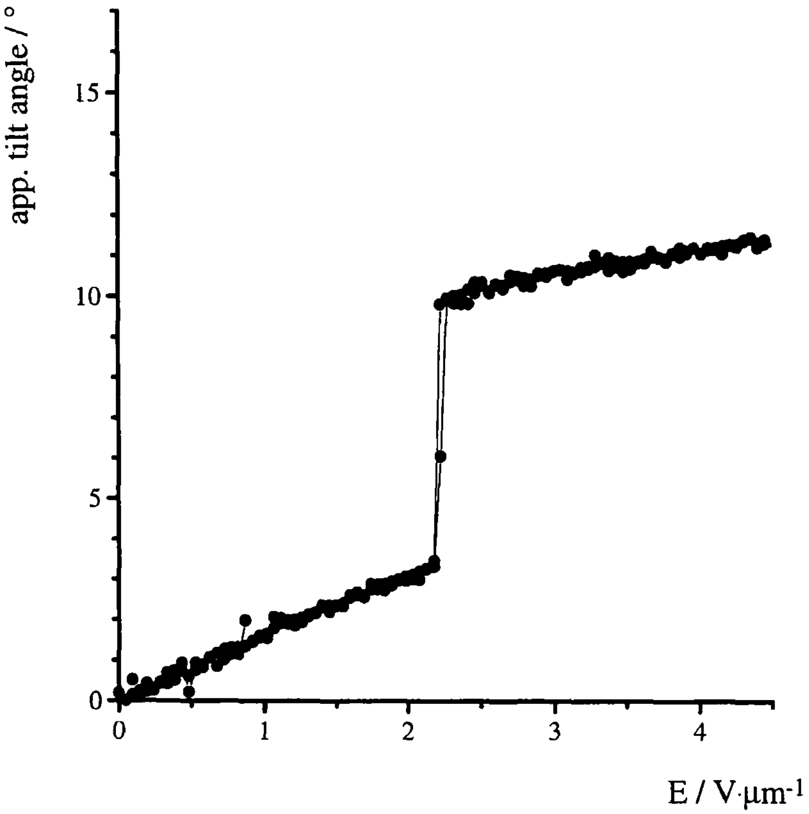

FIGURE 5 Apparent tilt angle of MHP8CBC as a function of electric field in the SmC^*_α phase (at 102°C).

Remarkable is the additional step of the optical tilt angle observed at an electric field strength of about 0.5 $V \cdot \mu m^{-1}$. The height of this step decreases with decreasing temperature and the step disappears at the SmC^*_x to SmC^*_γ transition temperature. At field strengths between 0.7 and 1.3 $V \cdot \mu m^{-1}$ a plateau of the apparent tilt with a value of about one third of the saturated tilt is reached.

Similar to the SmC^*_γ phase the dielectric spectrum of the SmC^*_x phase shows an absorption (Goldstone mode) at low frequencies. The magnitude of this absorption appears to be lower than in the SmC^*_γ phase. Whereas in the SmC^*_γ phase no absorption in the high frequency region has been found two additional relaxation processes occur in the SmC^*_x phase (in Fig. 10 denominated as mode 1 and mode 2). The origin of this two high frequency relaxation processes is unclear.

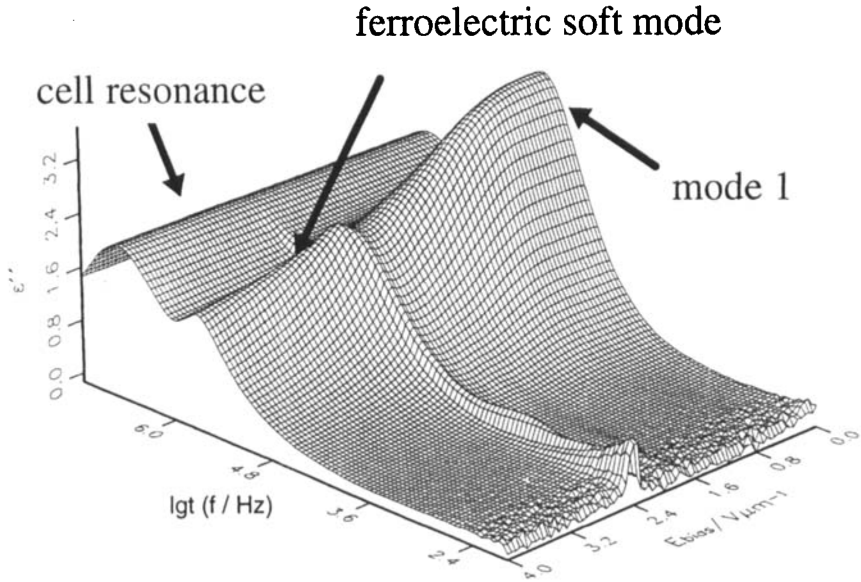

FIGURE 6 Dielectric loss of MHP8CBC versus frequency and electric field strength in the SmC_α^* and phase (at 102°C).

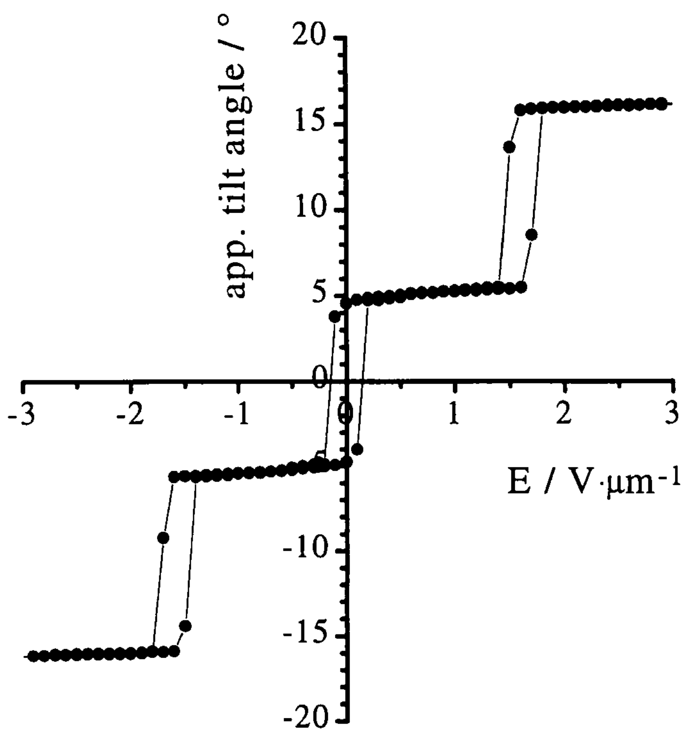

FIGURE 7 Apparent tilt angle as a function of electric field in the SmC_γ^* phase (at 107.5°C).

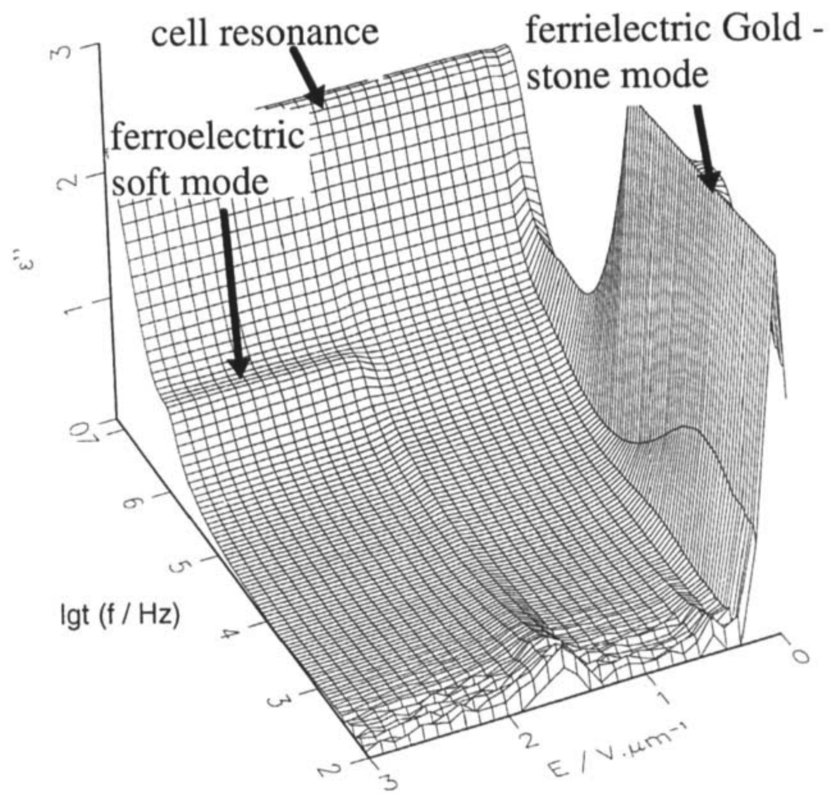

FIGURE 8 Dielectric loss versus frequency and electric field strength in the SmC^*_γ phase (at 107.5°C).

The dependence of the optical tilt angle on electric field with its different switching processes is in good agreement with the voltage dependence of the dielectric behaviour. When lowering the electric field strength, starting in the homogeneously tilted ferroelectric state, the first transition in the apparent tilt angle appears at about $1.3\,V \cdot \mu m^{-1}$. This coincides with the disappearance of the ferroelectric softmode in the dielectric spectra. The dielectric process denominated mode 2 exists in the voltage region between 0.7 and $1.3\ V \cdot \mu m^{-1}$ in which the plateau in the optical tilt is observed. The strong increase of the dielectric strength (from $\Delta\varepsilon \approx 2$ to $\Delta\varepsilon \approx 5$) at about $0.6\ V \cdot \mu m^{-1}$ is most likely connected with the stepwise decrease of the optical tilt to a value below one third of the saturated tilt. When further decreasing the electric field (to a value of about $0.2\ V \cdot \mu m^{-1}$) the reformation of the helical structure and the strong low frequency absorption described above is observed.

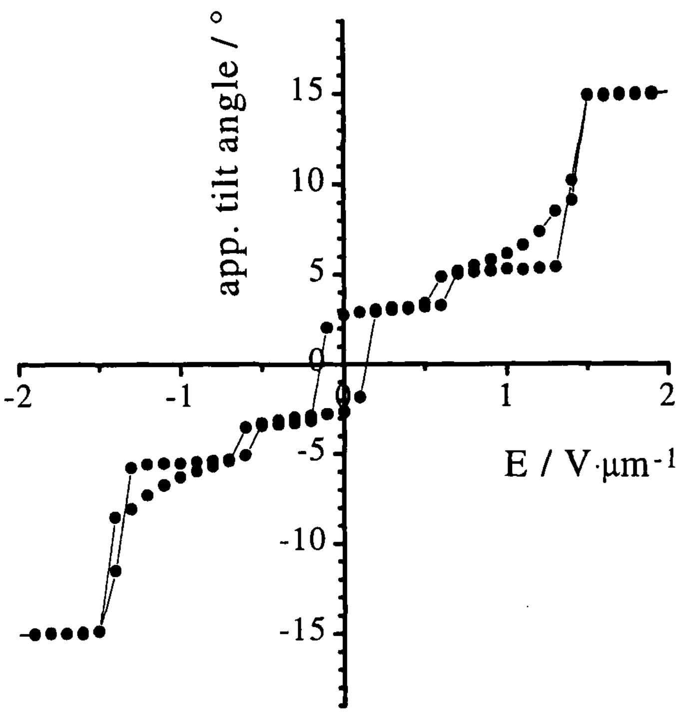

FIGURE 9 Apparent tilt angle as a function of electric field in the SmC$^*_\chi$ phase (at 108.5°C).

SmC$^*_A$ Phase

The electro-optical and dielectric properties of the SmC$^*_A$ phase under application of an electric field have been investigated for the compounds MHP8CBC and MHP9CBC. As shown in Figures 11 and 12 for both compounds down to 10 K below the phase transition into the SmC$^*_A$ phase an additional step in the electric field dependence of the apparent tilt appears. This step is due to the occurrence of an induced ferrielectric (in the following designated as FI) state.

With decreasing temperature the threshold of the switching process from the antiferroelectric (AF) into the FI state increases stronger than the threshold for the switching into the ferroelectric (F) state. Consequently the fieldinduced FI state disappears at a definite temperature and a direct switching from the antiferroelectric into the ferroelectric state is observed. Whereas in case of MHP8CBC the switching process FI↔F is hystereses free and only the switching AF↔FI shows a hystereses with a width of

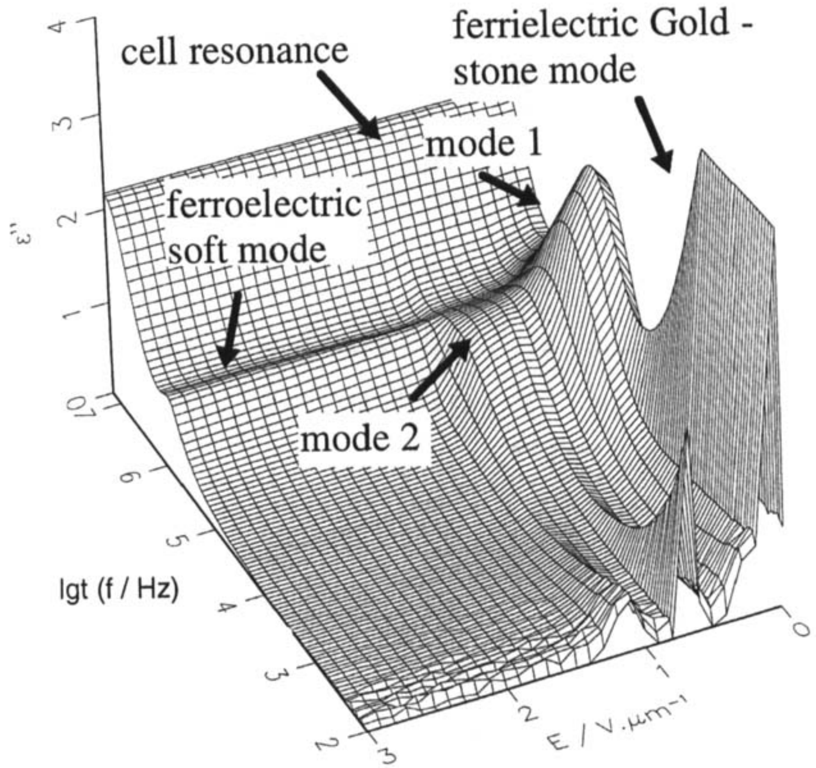

FIGURE 10 Dielectric loss versus frequency and electric field strength in the SmC_x^* phase (at 108.5°C).

about 1 $V \cdot \mu m^{-1}$, both processes are afflicted with a hystereses in case of MHP9CBC. In both substances the ratio of the apparent tilt angle of the ferrielectric state and the saturated value is nearly constant over the whole temperature range and shows a value of about one third.

As can be seen in Figure 13 the pentastate switching observed by tilt and polarization measurements is reflected in the dielectric spectra of both compounds which will be discussed on the basis of the spectrum of MHP8CBC 4 K below the SmC_α^* – SmC_A^* phase transition.

There are two absorptions at zero bias field which are typical for the SmC_A^* phase [9]. The dielectric strength of the high frequency mode (mode 2, $f \approx 0.5$ MHz) increases with increasing electric field strength from a value of about 1.7 until it reaches a maximum ($\Delta\varepsilon \approx 3.1$) just before switching to the FI-state takes place. After this it decreases rapidly reaches a plateau within the FI-state ($\Delta\varepsilon \approx 0.8$) and is totally quenched at the transition to the F-state. The low frequency mode (mode 1, $f \approx 20$ kHz) shows a similar

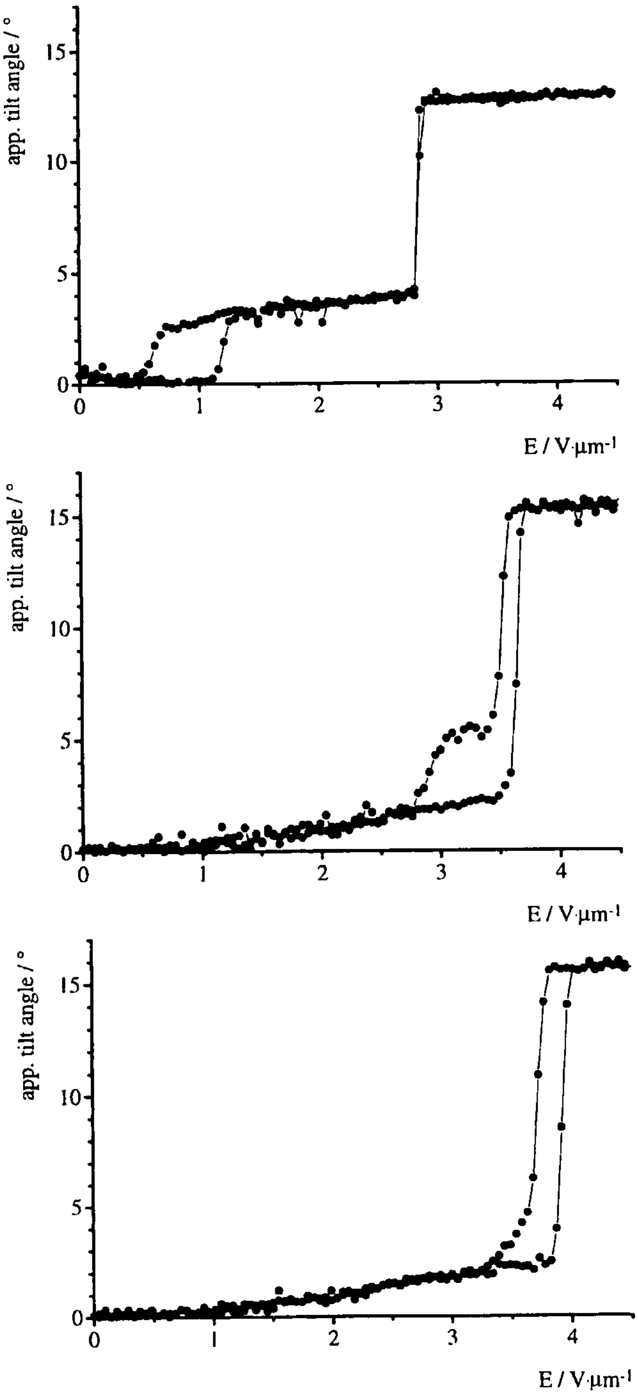

FIGURE 11 Apparent tilt angle of (S)-MHP8CBC as a function of electric field in the SmC_A^* phase (2, 10 and 12 K below the SmC_α^* – SmC_A^* phase transition).

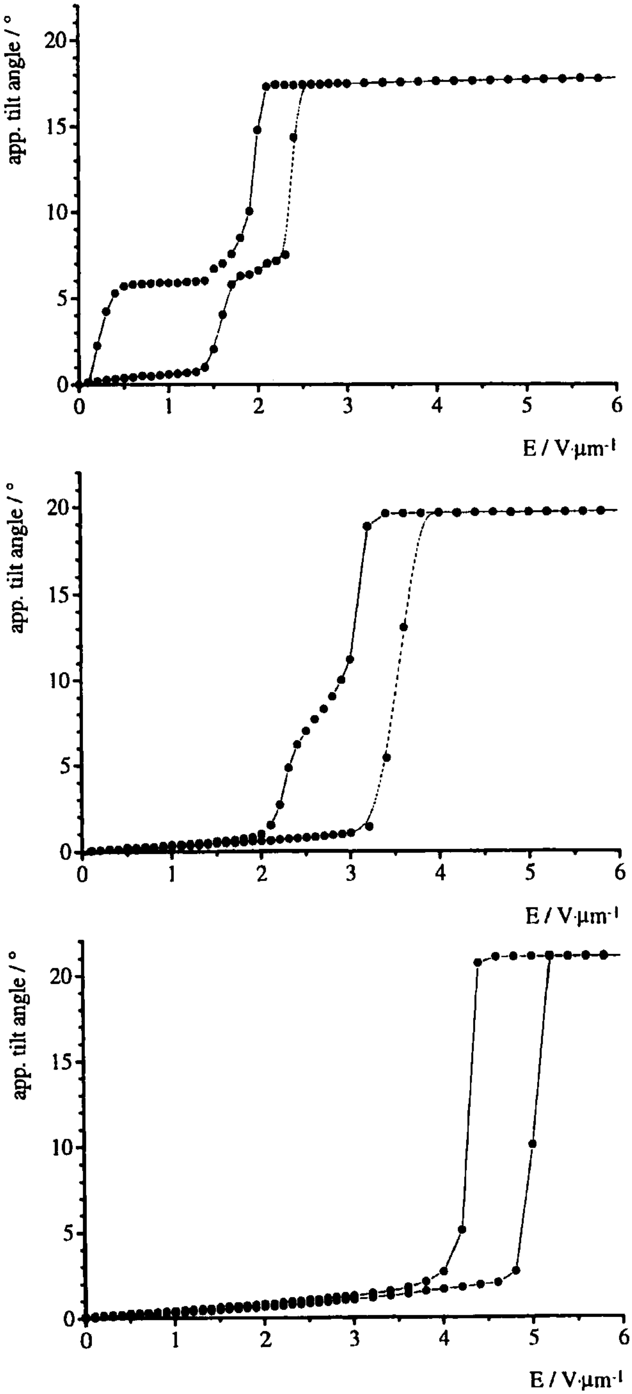

FIGURE 12 Apparent tilt angle of (S)-MHP9CBC as a function of electric field in the SmC_A^* phase (2, 10 and 24 K below the SmC_γ^* – SmC_A^* phase transition).

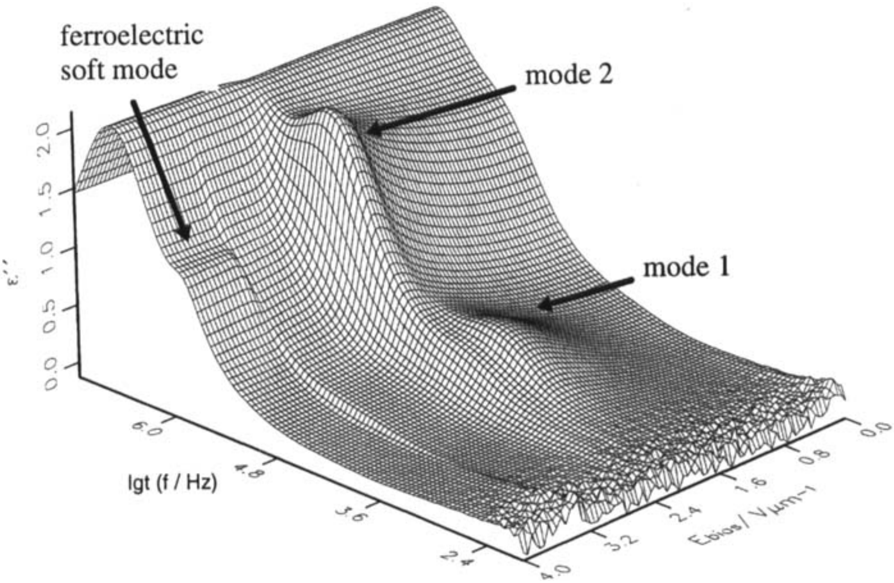

FIGURE 13 Dielectric loss ε'' of MHP8CBC 4 K below the SmC^*_α – SmC^*_A phase transition vs. frequency and dc electric field.

behaviour but the dielectric strength is about three times smaller than that of the high frequency mode. Decreasing the electric field strength in both modes a hystereses behaviour can be seen similar to that of the apparent tilt angle. Lowering the temperature the maximum of mode 2 shifts to higher values of the electric field until it coincides with the switching to the ferroelectric state where the absorption is quenched. Whereas the maximum of the high frequency mode shows the same temperature dependence as the threshold field of the switching AF↔FI, the maximum of mode 1 cannot be correlated with this transition.

ELECTRIC FIELD–TEMPERATURE PHASE DIAGRAM OF MHP8CBC

Summarizing the results of the electro-optical investigations by evaluating the different threshold field strengths allows us to construct the electric field–temperature phase diagram which is shown in Figure 14 for the compound MHP8CBC. In principle the SmC^*_A phase of both compounds exhibits a similar behaviour, e.g., a broad range of field induced ferrielectric

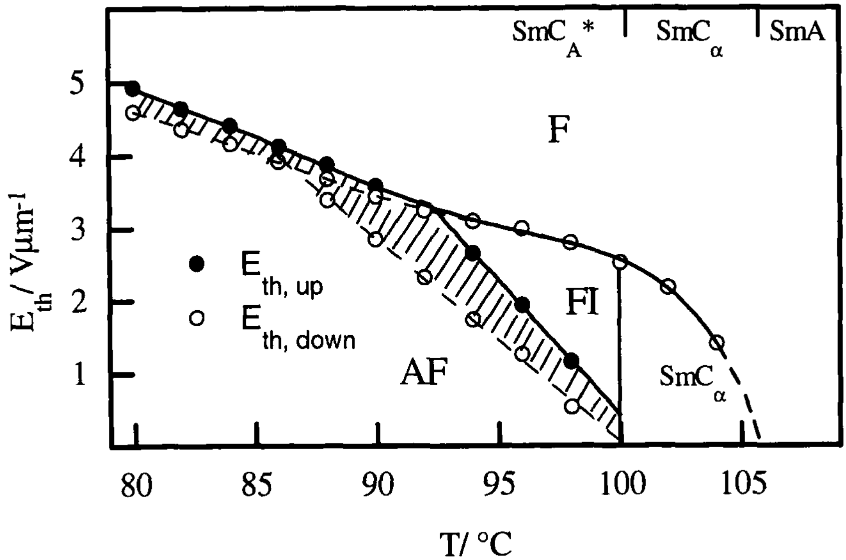

FIGURE 14 Electric field–temperature phase diagram obtained by evaluating the measurements of apparent tilt angle on increasing field strength (filled circles) respectively on decreasing field strength (empty circles). The phase sequence at zero field is given in the upper part of the diagram.

state. The main difference is the more complicated phase sequence of MHP9CBC in the temperature region above the SmC_A^* phase. Therefore, we will restrict our discussion on the properties of MHP8CBC which shows the phase sequence SmI_A^* – SmC_A^* – SmC_α^* – SmA – I. In the shaded regions of Figure 14 the ferrielectric respectively the ferroelectric state exist only when decreasing the electric field, e.g., giving a measure for the broadness of the hysteresis.

As described above the field induced ferrielectric phase is also detectable in the dielectric spectra evaluating the dependence of the dielectric loss on the applied DC electric field. Threshold fields of the transitions obtained from the dielectric spectra are in very good agreement with the values obtained by the measurements of the apparent tilt.

DISCUSSION

By miscibility studies it is proved that the compound MHP9CBC exhibits a smectic phase (SmC_x^* phase) in the temperature range between the SmC_α^*

phase and the SmC_{γ}^{*} phase which is not miscible with any of the smectic phases of the reference compound MHPOBC. This phase is clearly induced by chirality and shows a Schlieren texture with strong fluctuations of·the helical pitch in homeotropically aligned samples.

From the results of electro-optical and dielectric investigations one can summarize that the SmC_{x}^{*} phase of MHP9CBC shows ferrielectric properties but additionally exhibits a behaviour which is distinguishable from that of the SmC_{γ}^{*} phase. Like in the SmC_{γ}^{*} phase a low frequency absorption is observed in the dielectric spectrum of the SmC_{x}^{*} phase, which is probably due to the Goldstone-mode. On the other hand two additional relaxation processes with unknown molecular origin in the high frequency region have been found. An additional step of the optical tilt angle showing an increasing magnitude with increasing temperature is observed in the SmC_{x}^{*} phase. The value of the tilt at voltages below this step is smaller than one third of the saturated value and temperature dependent. Due to this temperature dependence one can conclude that there exists no fixed ratio between ferroelectric (homogeneously tilted) and antiferroelectric (alternating tilted) layer structures in the SmC_{x}^{*} phase, as it should be the case if the SmC_{x}^{*} phase would belong to a series of phases in the framework of a devil staircase (fixed ratio of ferro- and antiferroelectric layers in each phase) [11].

Taking into account these experimental results which are indicating a quite different physical behaviour of the SmC_{x}^{*} phase compared to that of the SmC_{γ}^{*} one can assume that both phases are not isostructural. Therefore it seems difficult to assume a structure for the SmC_{x}^{*} phase which is similar to the SmC_{γ}^{*} phase only exhibiting the opposite handiness of the helical structure as reported for the SmC_{FI1}^{*} and SmC_{FI2}^{*} phase of chiral tolans [10].

In order to get more information on the structure of the SmC_{x}^{*} phase further investigations have to be carried out.

References

[1] M. Fukui, H. Orihara, Y. Qamada, N. Qamamoto and Y. Ishibashi, *Jpn. J. Appl. Phys.*, **28**, L849 (1989).
[2] A. D. L. Chandani, E. Gorecka, Y. Ouchi, H. Takezoe and A. Fukuda, *Jpn. J. Appl. Phys.*, **28**, L1256 (1989).
[3] A. D. L. Chandani, T. Hagiwara, Y. Suzuki, Y. Ouchi, H. Takezoe and A. Fukuda, *Jpn. J. Appl. Phys.*, **27**, L729 (1988).
[4] E. Gorecka, A. D. L. Chandani, Y. Ouchi, H. Takezoe and A. Fukuda, *Jpn. J. Appl. Phys.*, **29**, 131 (1990).
[5] Y. Takanishi, K. Hiraoka, V. K. Agarwal, H. Takezoe, A. Fukuda and M. Matsushita, *Jpn. J. Appl. Phys.*, **30**, 2023 (1990).
[6] A. Fukuda, Y. Takanishi, T. Isozaki, K. Ishikawa and H. Takezoe, *J. Mater. Chem.*, **4**(7), 997 (1994).

[7] M. Cepič, G. Heppke, J.-M. Hollidt, D. Lötzsch, D. Moro and B. Žekš, *Mol. Cryst. Liq. Cryst.*, **263**, 207 (1995).
[8] T. Isozaki, Y. Suzuki, I. Kawamura, K. Mori, N. Yamamoto, Y. Yamada, H. Orihara and Y. Ishibashi, *Jpn. J. Appl. Phys.*, **30**, L1573 (1991).
[9] M. Buivydas, F. Gouda, S. T. Lagerwall and B. Stebler, *Liq. Cryst.*, **18**, 879 (1995).
[10] P. Gisse, V. L. Lormann, J. Pavel and H. T. Nguyen, *Ferroelectrics*, **178**, 297 (1996).
[11] T. Isozaki, T. Fujikawa, H. Takezoe, A. Fukuda, T. Hagiwara, Y. Suzuki and I. Kawamura, *Phys. Rev. B*, **48**(18), 13439 (1993).